Bistatic SAR Processing using Non-Linear Chirp Scaling

Yew Lam Neo[(1)], Ian Cumming[(1)], Frank Wong[(2)]

[(1)] Dept. of Electrical and Computer Engineering
The University of British Columbia
Vancouver, BC,V6T 1Z4,Canada
Email: nyewlam@dso.org.sg, ianc@ece.ubc.ca

[(2)] MacDonald Dettwiler and Associates
13800 Commerce Parkway,
Richmond, BC V6V 2J3,Canada.
Email: fhw@mda.ca

ABSTRACT

Non-Linear Chirp Scaling is an innovative way to focus bistatic SAR images and has been demonstrated to work on the configuration where the receiver is stationary and the transmitter imaging on broadside. This paper improves and extends the method to the configuration where both the receiver and the transmitter are imaging at a squint angle and moving in a parallel track with the same velocity. Simulated point targets using flight configurations similar to the airborne ONERA/DLR bistatic SAR experiments are used to verify the focusing algorithm.

KEYWORDS

Bistatic SAR processing, Non-Linear Chirp Scaling, parallel tracks.

INTRODUCTION

Traditional monostatic algorithms, such as the Range Doppler and Chirp Scaling algorithms, may not work well in a bistatic environment. A review of existing bistatic SAR algorithms such as wavenumber algorithm [1] and the Back Projection Algorithm [2] similar to the monostatic ω-k algorithm was conducted and it was concluded that Non-Linear Chirp Scaling algorithm [3] showed promising results. This paper extends and improves the existing Non-Linear Chirp Scaling algorithm to focus a bistatic image where both platforms moving in a parallel track with the same velocity

A joint X-band bistatic SAR experiment by ONERA/DLR [4] was carried out to explore the challenges associated with bistatic radar. It involves the use of two separate monostatic SAR systems carried by E-SAR and RAMSES, imaging at broadside. Two separate configurations were used in their experiments, both involving parallel flight paths and low squint angles. The algorithm developed in this paper can be used to focus both cases.

BISTATIC IMAGING MODEL

Bistatic SAR Imaging Geometry

Bistatic SAR has separate transmitter and receiver sites, whereby each platform can assume different velocities and different flight paths, as shown in Fig. 1. Together with the target, these three sites form the vertices of the bistatic triangle that lies in the bistatic imaging plane. The angle between the line of sight of the transmitter and the line of sight of the receiver forms the bistatic angle β. The baseline is the line joining the transmitter and the receiver.

In the configuration considered, the transmitter works in stripmap mode while the receiver steers its antenna footprint to match the transmitter antenna footprint.

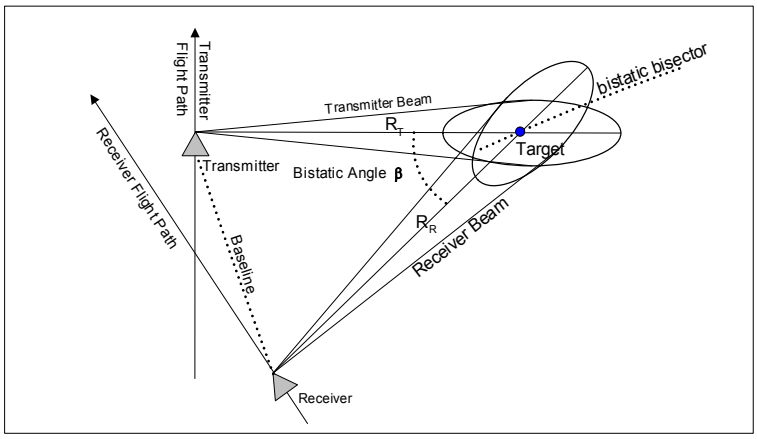

Fig. 1. Imaging Geometry of Bistatic SAR

NON-LINEAR CHIRP SCALING ALGORITHM

Existing Non-Linear Chirp Scaling Algorithm

Fig. 2 illustrates the main steps taken in the NLCS Algorithm [3], the residual QRCMC (Quadratic Range Cell Migration) is not part of the algorithm. The first step of the algorithm is range compression. Target trajectories after range compression have Linear Range Cell Migration (LRCM) which varies with range. However, this variation of LRCM is small; this is especially so for short wavelength systems. LRCM correction using a linear interpolation step is applied after range compression, targets with different FM rate (since they have different closest range of approach) fall into the same range gate. NLCS is applied to equalize the FM rates along each range cell by using a perturbation function. Once the azimuth FM rate is equalized for all range gates, azimuth compression can be carried out in the frequency domain to focus the image.

Extension to NLCS Algorithm

In the NLCS algorithm reported in [3], simulated point target experiments were documented for a monostatic case and a simple bistatic case where the receiver is stationary and the transmitter antenna pointing at zero Doppler. We have extended the algorithm to include parallel flight cases with moderate squint and incorporated a residual QRCM correction in the NLCS processing. This step is performed in the range Doppler domain after Non-Linear Chirp Scaling. Using a similar approach as given in [3], the perturbation function is cubic in azimuth time η and is given by:

$$h_{pert} = \exp(j\pi\alpha\eta^3) \tag{1}$$

and the coefficient α is given by

$$\alpha = \left(\frac{V_T^{\,2}\cos^2\theta_{sqT}K_T}{3\lambda R_T^{\,2}} + \frac{V_R^{\,2}\cos^2\theta_{sqR}K_R}{3\lambda R_R^{\,2}}\right) \tag{2}$$

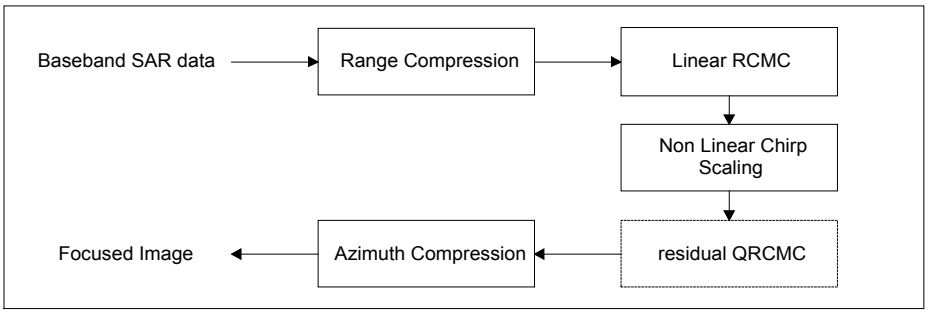

Fig. 2. NLCS Algorithm

where R_R is the slant range to the target at the time it is illuminated by the receiver beam centre, R_T is the slant range to the target at the time it is illuminated by the transmitter beam centre, V_T is the transmitter velocity and V_R is the receiver velocity. For this geometry, the squint angle of the receiver θ_{sqR} and squint angle of transmitter θ_{sqT} are constants.

The values K_T and K_R are proportional to the LRCM contribution by the transmitter and receiver respectively and are approximated by:

$$K_T = \frac{R_{Tcen}}{R_{cen}}(V_R \sin\theta_{sqR} + V_T \sin\theta_{sqT}) \tag{3}$$

and

$$K_R = \frac{R_{Rcen}}{R_{cen}}(V_R \sin\theta_{sqR} + V_T \sin\theta_{sqT}) \tag{4}$$

where R_{cen} is the round trip range to the centre of the image. R_{Tcen} is the transmitter portion and R_{Tcen} is the receiver portion.

$$R_{cen} = R_{Rcen} + R_{Tcen} \tag{5}$$

For the existing algorithm, the residual QRCM is left uncorrected and the algorithm breaks down when residual QRCM is greater than 1 range cell, causing significant IRW broadening. A residual quadratic range cell migration correction has been added (see Fig. 2) to address this limitation. By correcting the QRCM, the image focusing can be extended to higher resolution images and systems with longer wavelengths such as S-band and C-band systems.

In Fig. 3, the impulse responses come from a simulated C-band configuration with a residual QRCM of 1.66 samples. Without applying residual QRCM, there is a broadening of 7.4% in the range impulse response and broadening of 9.7% in the azimuth impulse response. With residual QRCM applied, the broadening in range is reduced to 2.8% and the azimuth broadening is reduced to 1.6%.

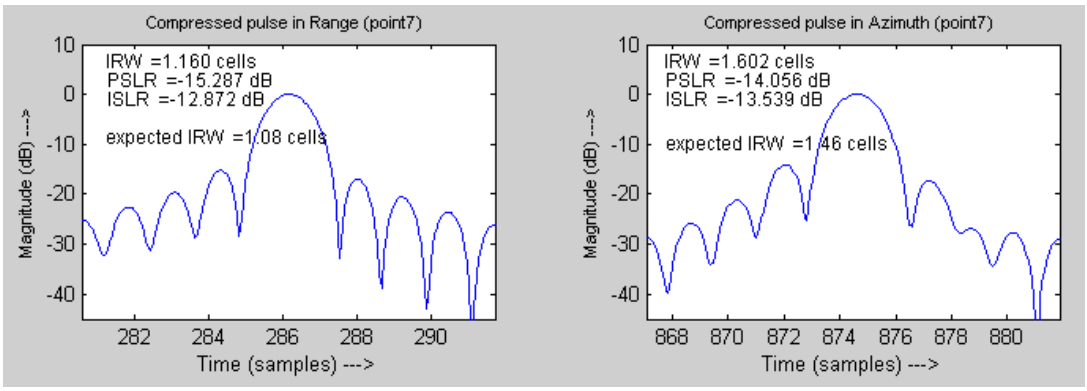

Fig. 3a. Impulse response without residual QRCMC

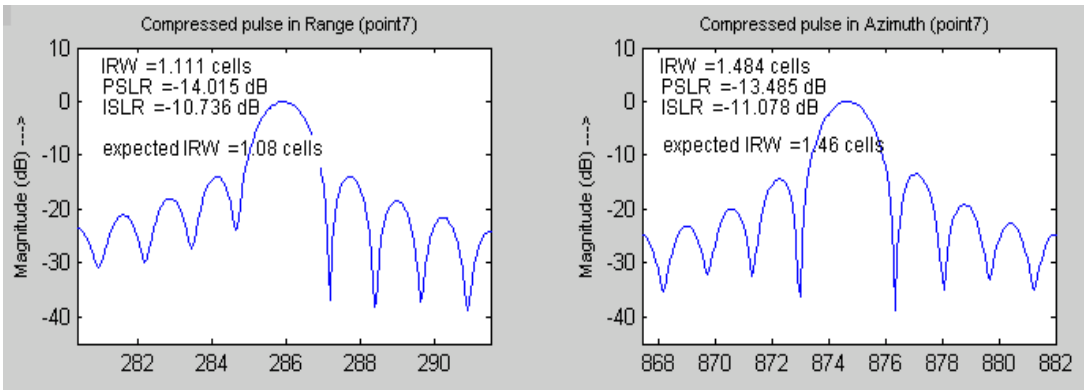

Fig. 3b. Impulse response with residual QRCMC

The extended NLCS algorithm presently uses a one dimensional azimuth time domain matched filter to do the compression. The computational load of the algorithm was found to be in the same order as monostatic algorithms such as accurate ω-k algorithm.

SIMULATION RESULTS

Parallel Tracks, Same Velocity

A simulation experiment was conducted on the point targets imaged at C-band with the transmitter and receiver 10 km apart with a transmitter squint of 25^o and receiver squint of 37.3^o. Transmitter is at an altitude of 10 km and Receiver is at an altitude of 6 km. Transmitter and receiver are laterally separated by 7 km and the receiver is slightly forward at 1km. Both platforms fly at 200m/sec. Bistatic angle is 13.03^o. Imaging 9 point targets arranged in a squared grid 600m as shown.

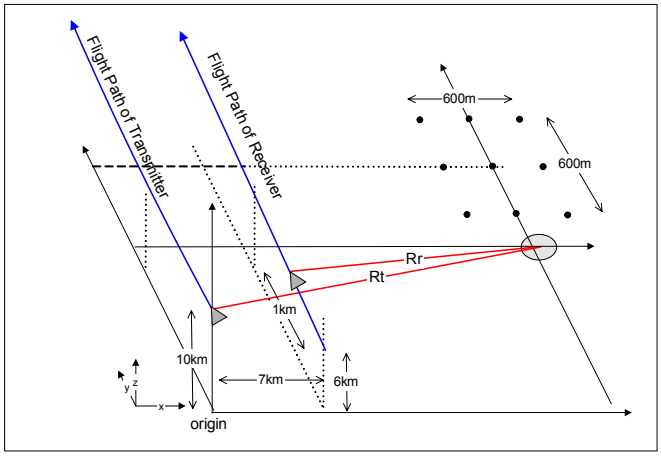

Fig. 4. Flight geometry of simulated case

The IRW of focused image has an error of less than 3 percent, the PSLR has an error of less than 1dB and ISLR has an error of 1.2dB when compared with the theoretical values. With QRCM left uncorrected, the IRW degrades by between 5 to 30 percent while PSLR has an error greater than 5.4dB and ISLR has an error of greater than 2.1dB. Thus, the new method has a better focusing ability.

ONERA/DLR EXPERIMENTS

Flight configuration similar to DLR experiment

The DLR configuration is shown in Fig. 5; both planes are flying along the same track in a typical “refuelling formation”.

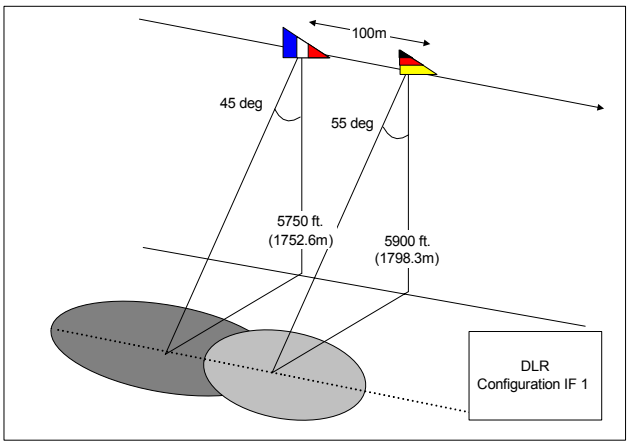

Fig. 5. Flight geometry of simulated case

A composite (round-trip) antenna pattern that has to be simulated in order to estimate the effective squint angles of the configuration correctly, since the centre of each antenna beam is pointing at different locations at the same time (see Fig. 6). Squint angles are measured to the centre of the composite beam, these angles are necessary for the LRCM correction and for Doppler centroid estimation. Using the composite antenna pattern simulated, the average squint angle for the transmitter is estimated to be -0.46^{o} while the receiver squint angle is 1.48^{o}. Without using the composite antenna, the transmitter squint and receiver squint would be recorded at zero squint. As shown in Table 1, the impulse response using the corrected squint angle shows a slightly better response when the composite antenna pattern is used. The error will be more pronounced if the separation between the two platforms was larger.

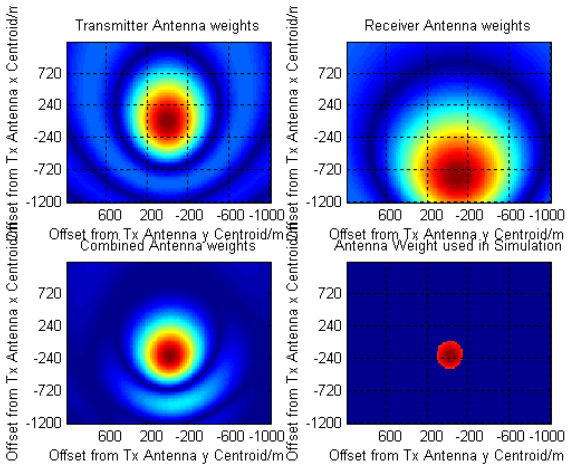

Fig. 6. Composite Antenna Footprint

Table 1. Typical impulse response for simulated DLR data

Parameter:	Rg IRW	Az IRW	Az PSLR	Az ISLR
Theoretical	1.237	1.015	-14.8	-11.4.
with Comp. Ant.	0.90	2.29	0.79	2.00
w/o Comp. Ant.	1.00	2.54	1.00	2.54

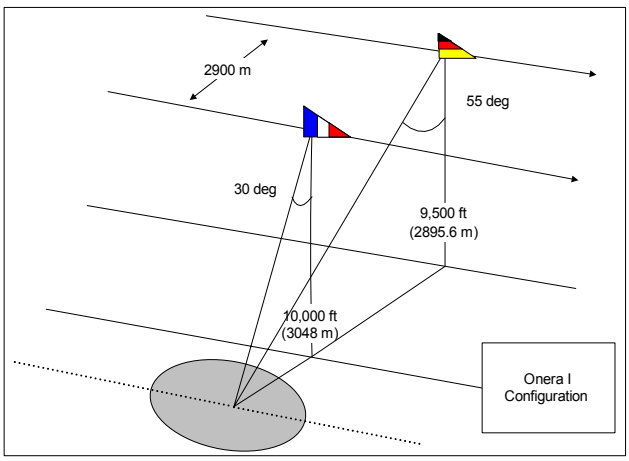

Fig. 7. Simulated ONERA Configuration

The ONERA configuration is shown in Fig. 7. The planes are flying in a parallel track configuration with a lateral distance of about 2 km. In this configuration, the image is less sensitive to the use of the effective antenna pattern. Simulation results shows that the algorithm developed can be used for the ONERA configuration as well.

CONCLUSIONS

Bistatic SAR has a number of complex geometries that makes the derivation of range equation difficult. We have analyzed some of the configurations and found the NLCS to be a useful algorithm. By deriving the perturbation function for the parallel track, same velocity configuration, we were able to focus the bistatic data. Applying residual QRCMC further improves the impulse response for this configuration.

REFERENCES

[1] M., Soumekh, "Bistatic synthetic aperture radar inversion with application in dynamic object imaging," in *IEEE Trans. on Signal Processing*, vol. 39, pp.2044-2055, Sep 1991.

[2] Y. Ding, D. C. Munson Jr., "Fast Back Projection Algorithm for Bistatic SAR Imaging," *IEEE ICIP*, vol II, pp 449-452. Sep 2002.

[3] F. H. Wong, and T. S. Yeo, "New Applications of Nonlinear Chirp Scaling in SAR Data Processing," in *IEEE Trans. Geosci. Remote Sensing*, vol. 39, pp. 946-953, May 2001.

[4] P. Dubois-Fernandez, et al., "ONERA-DLR Bistatic SAR Experiment: Design of the Experiment and Preliminary Results," in *Proc. Advanced SAR Workshop*, ASAR'03, Canadian Space Agency, Montreal, June 26-28, 2003.

GLOSSARY

IRW: Impulse Response Width

ISLR: Integrated Sidelobe Ratio

LRCM: Linear Range Cell Migration

NLCS: Non-Linear Chirp Scaling

PSLR: Peak Sidelobe Ratio

QRCM: Quadratic Range Cell Migration

SAR: Synthetic Aperture Radar